Improved Data Association for ICP-based Scan Matching in Noisy and Dynamic Environments

Diego Rodriguez-Losada and Javier Minguez

Abstract— **This paper presents a technique to improve the data association in the Iterative Closest Point [2] based scan matching. The method is based on a distance-filter constructed on the basis of an analysis of the set of solutions produced by the associations in the sensor configuration space. This leads to a robust strategy to filter all the associations that do not explain the principal motion of the scan (due to noise in the sensor, large odometry errors, spurious, occlusions or dynamic features for example). The experimental results suggest that the improvement of the data association leads to more robust and faster methods in the presence of wrong correspondences.**

I. Introduction

A key issue in autonomous mobile robots is to keep track of the vehicle position. When the robot is equipped with range sensors, one common framework is scan matching. The objective is to compute the relative motion of a vehicle between two consecutive configurations using the sensor measurements. Although these techniques are local in nature, many applications in robotics such as mapping, localization or tracking incorporate them to estimate the relative robot displacement [21], [9], [15], [11], [16].

Scan matching is an active research area that has produced many different techniques. Roughly, they can be divided in two groups. The first one deals with structured scenarios [8], [6], [4] and the other with raw data [3], [7], [2]. The latter does not assume any type of structure and estimates the sensor displacement by maximizing the overlap between the range measurements or scans. The most popular of these methods is the Iterative Closest Point (ICP) algorithm [2] (see [20] for variants of the original method). This method is based on an iterative process in two steps: first a set of correspondent points between the scans is computed and then, the sensor displacement is estimated by minimizing the error of the correspondences. This process is repeated until convergence.

The most critical point of the ICP is the establishment of the correspondences. Since no high level features are used, the computation of the joint matching of the points of both scans is computationally very expensive (exponential with the number of points of the scans). To reduce the complexity, the ICP-type algorithms use the nearest-neighbor rule to establish pairs of correspondences between the points of each scan (see [12], [19], [14], [17] for sophisticated

ways to compute the nearest-neighbor and ameliorate performance). This step is crucial for these techniques since the remaining of the strategy depends on their quality. Although these techniques work well in static environments, their performance degrades in situations where the correspondence process becomes more difficult: (i) noise in the sensor, (ii) large errors in the sensor odometry, (iii) spurious, (iv) new discovered areas, (v) occlusions and (vi) dynamic obstacles, among others. The contribution of this paper is an improved data association to ameliorate the scan matching performance under the previous conditions.

Some works have addressed this difficulty by evaluating the correspondence error as a measure of its goodness. For instance, a trimmed version of the ICP [5] simply discards the worst correspondences. Other strategy is to split the scans in sectors and discard those with a high mean correspondence error [1]. In [10] and [16], the scan matching is formulated as a an Expectation-Maximization and the effect of dynamic measurements is minimized through a weighting process. Unfortunately, wrong correspondences do not always have a large correspondence error, which affects the robustness and the convergence of previous approaches.

In this paper we analyze the set of solutions produced by the ICP correspondences in the configuration space of the sensor. This leads to a robust strategy to filter all the associations that do not explain the principal motion of the scan. The experimental results suggest that the improvement of the data association leads to more robust and faster methods in the presence of wrong correspondences.

The paper is organized as follows: in Section II we describe the ICP framework. Sections III and IV present the framework. In section V, we discuss the experimental results and we compare our method with existing techniques. Finally we draw our conclusions in Section VI.

II. Iterative Closest Point scan matching

The Iterative Closest Point algorithm addresses the scan matching problem with an iterative process in two steps. At each iteration k, there is a search of correspondences between the points of both scans (Z_{ref} and Z_{new}). Then, the estimation of relative displacement $\mathbf{q_0}$ is improved through a minimization process until convergence.

More precisely, let be a point $\mathbf{p} \in \mathbf{R}^2$ and a sensor configuration $\mathbf{q} = (x, y, \theta) \in \mathbf{R}^2 \times [-\pi, \pi]$. Let be $\{\mathbf{p_1} \dots \mathbf{p_{N_{ref}}}\}$ the points of reference scan Z_{ref} and $\{\mathbf{t_1} \dots \mathbf{t_{N_{new}}}\}$ the points of the other scan Z_{new} (expressed in the frame of Z_{ref} using $\mathbf{q_0}$). Let be $\mathbf{q_k} = \mathbf{q_0}$. Repeat:

1) For each $\mathbf{p_i}$ in Z_{ref} compute the closest point $\mathbf{r_j}$ in Z_{new} (transformed to the system of reference Z_{ref} using the estimation $\mathbf{q_k}$) whose distance is lower than a given threshold d_{min}:

$$\mathbf{r_i} = \arg\min_{\mathbf{t_j}}\{d(\mathbf{p_i}, \mathbf{t_j})\} \qquad (1)$$

The result is a set of N associations $A = \{(\mathbf{p_i}, \mathbf{r_i}) \mid i = 1 \ldots N\}$.

2) Compute the displacement estimation q_{min} that minimizes the mean square error between pairs of C:

$$E_{dist}(\mathbf{q}) = \sum_{i=1}^{N} d(\mathbf{p_i}, \mathbf{q}(\mathbf{r_i}))^2 \qquad (2)$$

Let be $\mathbf{q_{sol}} = \mathbf{q_{min}} \oplus \mathbf{q_k}$. If there is convergence the estimation is $\mathbf{q_{sol}}$, otherwise iterate again with $\mathbf{q_{k+1}} = \mathbf{q_{sol}}$.

As mentioned in the introduction, the critical point of this framework is the first step: the establishment of the correspondences. This is because the second step strongly depends on the quality of the set of associations. The noise in the sensor, large errors in the sensor odometry, spurious, new discovered areas, occlusions or dynamic obstacles could produce wrong associations affecting the robustness. That is why many existing scan matching techniques are of limited applicability under these working conditions.

The proposal of this paper is to introduce an intermediate step between the associations and the minimization. The idea is to filter those associations that do not explain the main motion of the scan and thus are likely to be wrong associations. The study of the associations is performed in the sensor configuration space. The next section addresses this study.

III. ASSOCIATIONS IN THE SENSOR CONFIGURATION SPACE

In this section we describe some properties of the associations in the sensor configuration space. Recall that we have a set $A = \{a_1 \ldots a_N\}$ of N associations. One association is $a_i = \{\mathbf{p_i}, \mathbf{r_i}\}$ such that $\mathbf{p_i} = (p_{ix}, p_{iy})$ and $\mathbf{r_i} = (r_{ix}, r_{iy})$. In the set A, p associations come from the *static structure*, m associations from the *dynamic obstacles* and d associations are *spurious* or *wrong*. In general $p > m+d$ (the static structure is predominant). We describe next how these associations are related in the sensor configuration space.

A. Basic problem: 1 association

The displacements $\mathbf{q}$ that solve one association $a = \{\mathbf{p}, \mathbf{r}\}$ hold:

$$\mathbf{p} = \mathbf{T} + \mathbf{R}(\theta)\mathbf{r} \qquad (3)$$

where $\mathbf{T} = (\mathbf{x}, \mathbf{y})$ and $\mathbf{R}(\theta)$ is the rotation matrix. Equation (3) can be written as:

$$f(x, y, \theta) = \mathbf{p} - (\mathbf{T} + \mathbf{R}(\theta)\mathbf{r}) \qquad (4)$$

Function $f(x, y, \theta)$ defines a one-dimensional manifold in the sensor configuration space $\mathbf{R}^2 \times [-\pi, \pi]$. This manifold

has the shape of a circular helix since Equation (4) can be rewritten as:

$$f(x, y, \theta) = (p_x + ||\mathbf{r}|| \cos(\theta + \beta), p_y + ||\mathbf{r}|| \sin(\theta + \beta), \theta) \quad (5)$$

where $\beta = \arctan\frac{-r_y}{r_x}$. The center of the helix is $\mathbf{p}$ and the radius $||\mathbf{r}||$. Notice that the set of solutions $\mathbf{q}$ for each association is an helix (C^∞) in the sensor configuration space.

Another tool that will be used later is the distance from a given configuration $\mathbf{q_0} = (x_0, y_0, \theta_0)$ to an helix f. In the configuration space, we define the norm of $\mathbf{q}$ as in [14]:

$$||\mathbf{q}|| = \sqrt{x^2 + y^2 + L^2\theta^2} \qquad (6)$$

where L is a positive real number homogeneous to a length. We define the distance from a configuration to an helix:

$$d_{qf}(\mathbf{q_0}, f)) = ||\mathbf{q_c} - \mathbf{q_0}||, \text{ such that } \mathbf{q_c} = \arg\min_{\mathbf{q}\in f} ||\mathbf{q} - \mathbf{q_0}||^2 \qquad (7)$$

Since f is a one dimensional manifold in θ (Equation (5)), the minimum of $||\mathbf{q} - \mathbf{q_0}||^2$ is given by:

$$\frac{\partial ||f(x, y, \theta) - \mathbf{q_0}||^2}{\partial\theta} = 0 \qquad (8)$$

Developing and using Equation (4) we have an expression of the form:

$$a\theta + b\sin\theta + c\cos\theta + d = 0 \qquad (9)$$

where: $a = L^2$, $b = \mathbf{pr}^T - x_0 p_{2x} - y_0 p_{2y}$, $c = p_{1x}r_{2y} - p_{1y}r_{2x} - x_0 p_{2y} + y_0 p_{2x}$ and $d = -\theta_0 L^2$. Unfortunately there is no closed form solution for Equation (9) thus we use Taylor $\theta \simeq \theta_l$:

$$\theta_{min} = \frac{(b\theta_l - c)\cos\theta_l - (c\theta_l + b)\sin\theta_l - d}{a + b\cos\theta_l - c\sin\theta_l} \qquad (10)$$

The linearization point is:

$$\theta_l = \arctan\frac{q_{0y} - p_y}{q_{0x} - p_x} - \arctan\frac{r_y}{r_x} \qquad (11)$$

computed as the projection of $\mathbf{q_0}$ to the cylinder that embeds the helix (Equation (5)). Substituting θ_{min} in Equation (5) we get $\mathbf{q_{min}}$. Finally:

$$d_{qf}(\mathbf{q_0}, f)) = ||\mathbf{q_{min}} - \mathbf{q_0}|| \qquad (12)$$

B. Proximity of Manifolds to a Region of Reference

Let say that we have a region of configurations of reference defined like a compact set embedded in the configuration space $\Omega \in \mathbf{R}^2 \times [-\pi, \pi]$. One evaluation of the goodness of an association a is to compute the distance to the manifold f of solutions to this set:

$$d_{Rf}(\Omega, f) = \min_{\mathbf{q}\in\Omega} d_{pf}(\mathbf{q}, f) \qquad (13)$$

where d_{pf} is the distance from a configuration to an helix. When the solution of reference is the motion of the sensor, then the distance of the manifolds that explain this motion to the solution is zero, while the other associations give a greater distance.
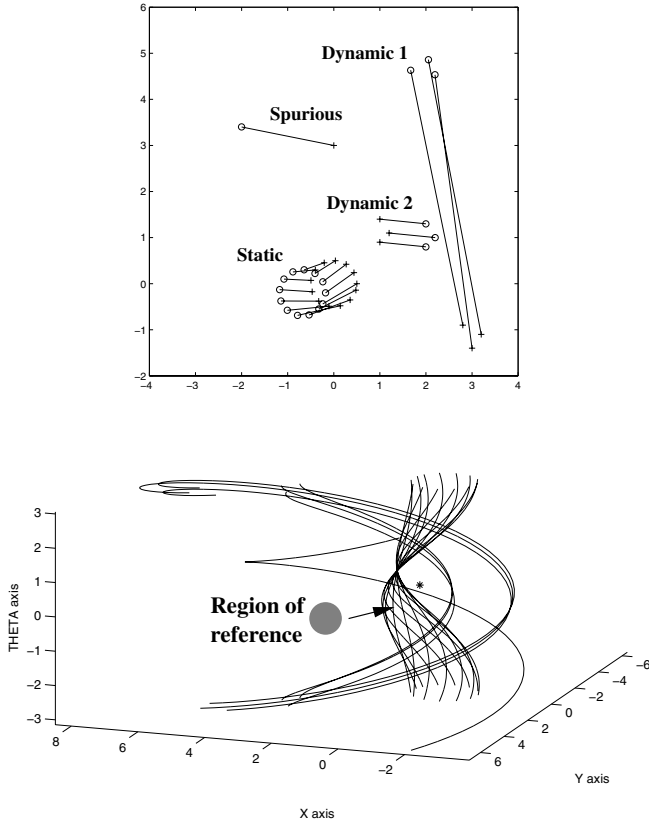
Fig. 1. This Figure shows a set of associations (top) and the curves that generate in the sensor configuration space (bottom). (Top) Two measurements with a given motion between them. The circle is static and there are two dynamic obstacles that have their motion plus the sensor motion. (Bottom) In the sensor configuration space, each association creates a curve of solutions. The *region of reference* is a set of configurations computed by a given method that explains the motion of the sensor. The curves closed to this set are created by associations of the static structure.

However, in realistic operation the measures are corrupted by noise. Although it is not describe here in detail due to space constraints, one can use continuity arguments in Equation (13) to demonstrate that when the noise tends to zero, the solution tends to the perfect solution (zero distance). In any case, the noise degrades the solution and thus the location of the manifolds. By computing the distance of the manifold to the solution of reference one have a robust criterion to deal with noise. Figure 1 shows an example.

This process is useful to evaluate associations if one can have in advance a good approximation of a region of configurations likely to explain the motion.

In summary, in this section we have described some properties of the associations in the configuration space and outlined one strategy to detect the static structure of the scenario based on the distance of the manifolds to a reference solution.

IV. THE PROPOSED FRAMEWORK

In the previous section we derived some tools to measure the distance from a given solution of reference to the set of solutions of each association. We show next how to use this
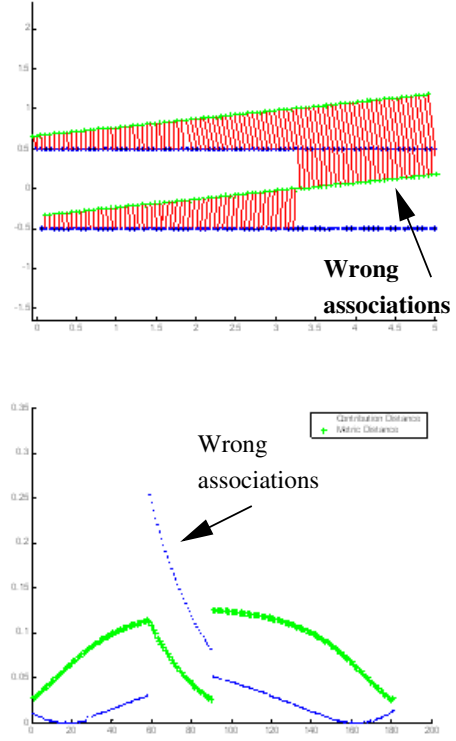

Fig. 2. (Top) Two scan and associations with the [?] distance. (Bottom). Metric and d_{Rf} distances. The wrong associations are detected since the d_{Rf} strongly increases.

distance to filter those associations likely to be incorrect. The strategy has two steps:

1) Computation of the solution of reference. In this step we apply the least squares (Equation (2)) with the initial set of associations A. The estimated solution is $\mathbf{q_{ref}}$ (solution of reference).
2) Filtering the associations. For all associations $a_i \in A$ we compute the $d_{Rf}(\mathbf{q_{ref}}, f_i)$. Then a given percentage is filtered. The remaining set is A'.

Both steps are carried out between steps 1 and 2 in the standard ICP framework (see Section II).

The idea underlying this approach is that with the first minimization, we obtain a coarse estimation of the sensor displacement. In this process, all the correspondences take part. In the next step, we evaluate all the manifolds by computing their distance to the reference solution. If this distance is small, this means that the set of solutions of this association is close to the solution of reference, and thus this association is likely to explain the same motion that the reference one. However, when the distance is large, the solution set is far to the reference solution. This means that this association comes from an spurious or wrong association and thus is rejected. At the end of this process we have a set A' of associations that explain a similar motion. Notice that A' is the set A but filtered with a criterion of distance in the space of solutions.
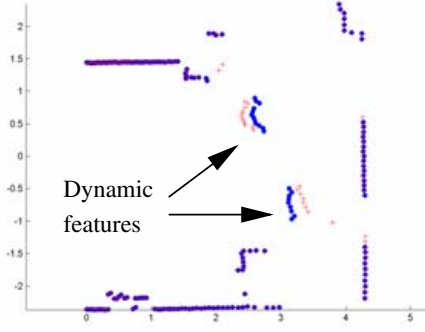
Fig. 3. Two range scans in a dynamic scenario.

We describe next an academic but illustrative example of this process. Figure 2 depicts a corridor and the same corridor but rotated a given quantity. The nearest-neighbor automatically process the associations computing the set A. Now we use the filtering strategy. The minimization is applied to compute $\mathbf{q_{ref}}$. The solution $\mathbf{q_{ref}}$ is just a coarse approximation to the motion due to the large number of wrong associations. Then we compute the distance of $\mathbf{q_{ref}}$ to each of the manifolds created by each association of A and we filter those with a distance greater than d_{th}. Notice how the wrong associations produce a distance that is significantly greater than the correct associations. Finally the minimization is applied to the set A' to get the solution $\mathbf{q_{min}}$ of this step of the ICP.

V. EXPERIMENTS

We have performed three types of experiments to evaluate the technique: (i) static scenario, (ii) dynamic scenario and a (iii) a run in the laboratory. The sensor is a SICK LMS200 mounted on a *B21r* robot. This sensor gathers 181 range measurements (with a field of view of $180°$) at 5Hz with a maximum range of 8.1 meters.

The objective of the experiments was to show how the filtering strategy of the previous sections improves the results of ICP methods in terms of convergence rate, precision and robustness under different conditions. We decided to modify the MbICP method [14] since it has been recently demonstrated that it improves widely used techniques such as [13], [2]. In the experiments we compared the performance of the ICP [2] and MbICP [14] with the MbICP equipped with the new data association (that we named MbICP-IDA).

In order to provide a fair comparison, we fixed the same settings for all methods. The maximum range was limited to 6m. We used a smooth criterion of convergence [19] that requires two consecutive iterations with a location correction lower than 0.0005 (m, rad) for each coordinate. The maximum number of iterations is 300. Furthermore, we set the maximum percentage of discarded associations to 20%.

A. Scan against scan experiments

In these experiments we evaluated the scan matching performance with two data sets: (i) an static scenario artifi-

cially corrupted with noise in the measurements and sensor displacement, and (ii) a dynamic scenario. The first dataset is composed by 879 laser scans acquired in a 60m trajectory along different kinds of scenarios: regular rooms, corridors, cluttered and open spaces, etc (Figure 4). Each scan is compared with itself, so ground truth is available $(0, 0, 0)$. To simulate sensor noise and outliers (reflections, occlusions, etc) each point is contaminated with uniformly distributed noise in the range ±0.025m, and a random 10% of the points are also contaminated with noise in the range ±0.50 m. For each scan 10 different initial random locations are generated (8790 runs for each range).

The second data set consists of 619 laser scans acquired in a fixed location with 2 or 3 people continuously walking in front of the robot (generating occlusions and non-static data points). Figure 3 shows an example. Each scan is compared with the next one, however, as the vehicle is static the ground truth is $(0, 0, 0)$. For each scan 10 different initial random locations are generated (6190 runs for each range).

The next two tables summarize the results.

TABLE I
MBICP +IDA VS MBICP AND ICP: STATIC SCENARIO

Static Scenario	Method	ICP	MbICP	MbICP + IDA
	Conv. Rate (#)	23.73	20.9	14.51
Sensor error	Precision (m)	0.011	0.007	0.007
$(0.15m, 0.15m, 17°)$	Robustness (%)	98.01	99.60	99.93
	Conv. Rate (#)	32.09	27.46	19.24
Sensor error	Precision (m)	0.011	0.007	0.007
$(0.3m, 0.3m, 34°)$	Robustness (%)	92.67	95.90	99.17

TABLE II
MBICP +IDA VS MBICP AND ICP: DYNAMIC SCENARIO

Dynamic Scenario	Method	ICP	MbICP	MbICP + IDA
	Conv. Rate (#)	26.51	22.41	17.02
Sensor error	Precision (m)	0.024	0.004	0.004
$(0.15m, 0.15m, 17°)$	Robustness (%)	52.73	80.64	86.00
	Conv. Rate (#)	37.359	30.24	22.13
Sensor error	Precision (m)	0.025	0.004	0.004
$(0.3m, 0.3m, 34°)$	Robustness (%)	47.15	78.25	85.01

We discuss first the results in terms of robustness. A run was considered a failure when the solution was larger than 0.02m in translation and 0.02rad in rotation (notice that the ground truth is $(0, 0, 0)$). These values are just a threshold used to identify failures of the method. In Table I we observe that all the methods are robust. However, as the noise in the sensor increases the robustness of the methods decreases. This effect also appears in the dynamic scenario since there are many issues involved like dynamic associations and occlusions affecting the correspondence step of the methods (see Table II). In any case, it is clear that the filtered data association improves the robustness in both cases.

The MbICP and the MbICP+IDA have the same order of precision. This is because precision is very related with the behavior of the method in the vicinity of the solution. Since this analysis is performed for the runs that converged,
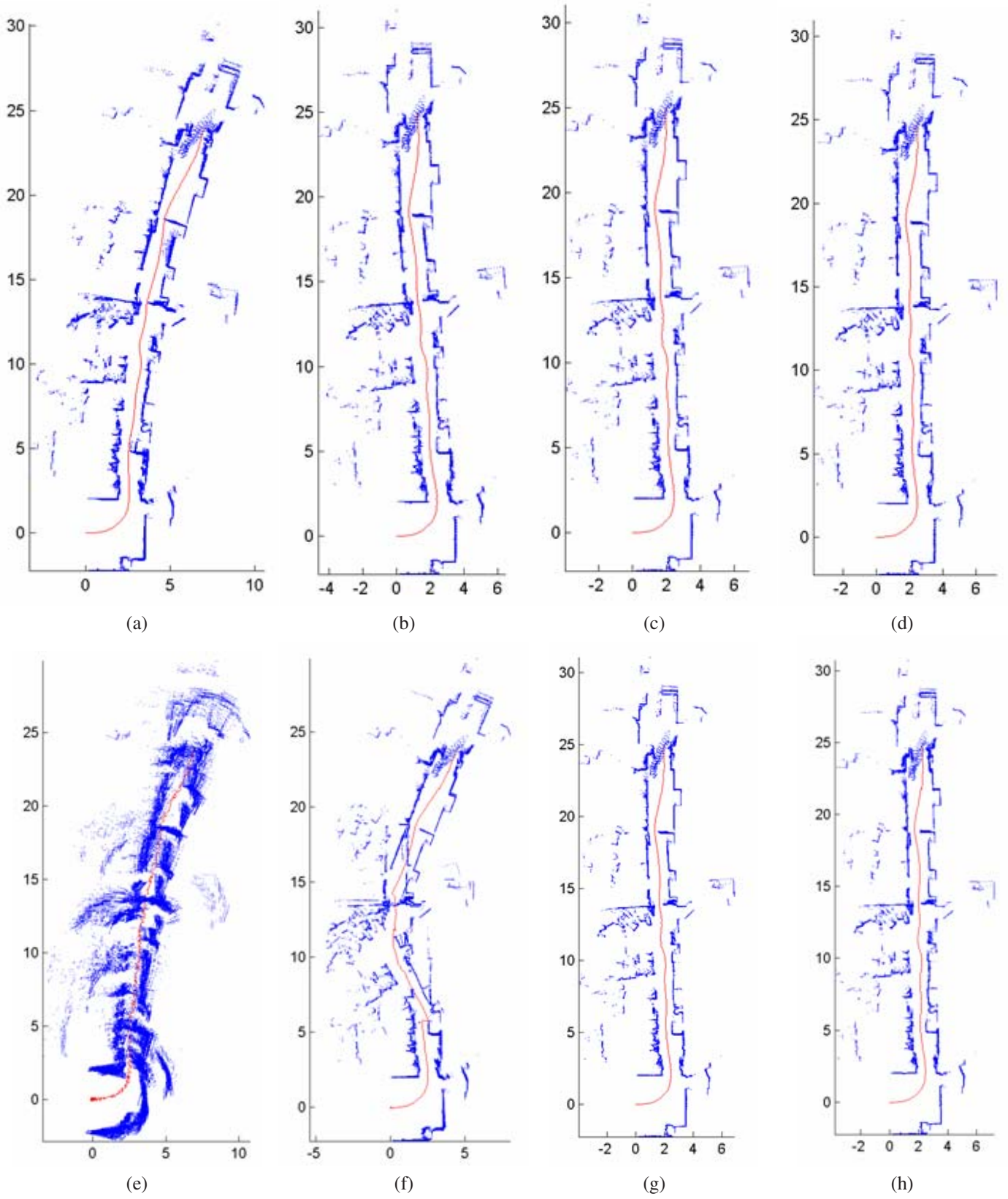
Fig. 4. Visual odometry. (Top) experiments with the odometry of the robot. (a) Odometry, (b) ICP, (c) MbICP and (d) MbICP+IDA. (Bottom) experiments with the odometry of the robot corrupted with noise. (a) Odometry, (b) ICP, (c) MbICP and (d) MbICP+IDA.

then the role of the new data association is not very relevant (almost no error in the sensor location).

The MbICP+IDA converges faster than the other methods. This was expected since the new data association improves the correspondences and thus the subsequent minimization. The computation time of the MbICP and the MbICP+IDA are very similar. This is because the computation time of the extra minimization is very small with respect to the data association step.

In summary the MbICP with the new data association outperforms the standard methods in robustness, precision and convergence. This is because the proposed approach filters the incorrect data associations in the presence of large error locations, occlusions, dynamic objects, etc.

B. Visual map with scan matching

The second test corresponds to the matching of consecutive scans of the first data set. As the ground truth is not available, the validation is done by plotting all the scans using the locations estimated by the methods.

Firstly, we tested the method using the robot odometry (top of Figure 4). However there is no a large difference between the maps. Only the map of the MbICP+IDA is slightly straighter than the map of the MbICP and the ICP. This is due to the better robustness of the MbICP+IDA. The convergence rates (the average number of iterations) are 6.00, 6.06 and 6.14 for the MbICP+IDC, MbICP and ICP respectively. There is no a significant difference since the odometry is quite good.

We repeated the experiments by corrupting the sensor location with uniformly distributed noise in the range $\pm(0.15m, 0.15m, 17°)$. Then the scan matching process is much more difficult. Bottom Figure 4 shows the visual maps obtained. Again the results are very similar for both methods. However, again the MbICP+IDA performs slightly better due to the improved data association. The convergence rates are 15.73, 18.35 and 19.86 for the MbICP+IDA, MbICP and the ICP respectively. This shows a reduction in the required number of iterations.

VI. Conclusions

This paper presents a technique to improve the data association in the ICP-based scan matching. The method is based on a distance-filter constructed on the basis of an analysis of the set of solutions produced by the associations in the sensor configuration space. This leads to a robust strategy to filter all the associations that do not explain the principal motion of the scan greatly improving the next steps of the methods. The experimental results suggest that the improvement of the data association leads to more robust and faster method in the presence of wrong correspondences.

Future work will concentrate in improving the rejection criterion with adaptive thresholds. Furthermore, we will investigate the usage of clustering strategies in the sensor configuration space of each pairing to explicitly classify scan points as static, dynamic, non-visible structure and outliers.

References

[1] O. Bengtsson and A.-J. Baerveldt. Localization in changing environments by matching laser range scans. In *EURobot*, pages 169–176, 1999.

[2] P. Besl and N. McKay. A method for registration of 3-d shapes. *IEEE Transactions on Pattern Analysis and Machine Intelligence*, 14:239–256, 1992.

[3] P. Biber and W. Straßer. The normal distributions transform: A new approach to laser scan matching. In *IEEE Int. Conf. on Intelligent Robots and Systems*, Las Vegas, USA, 2003.

[4] J. A. Castellanos, J. D. Tardós, and J. Neira. Constraint-based mobile robot localization. In *Advanced Robotics and Intelligent Systems*, IEE, Control Series 51, 1996.

[5] D. Cheverikov, D. Svirko, and P. Krsek. The trimmed iterative closest point algorithm. In *International Conference on Pattern Recognition*, volume 3, pages 545–548, 2002.

[6] I. Cox. Blanche: An experiment in guidance and navigation of an autonomous robot vehicle. *IEEE Transactions on Robotics and Automation*, 7:193–204, 1991.

[7] J. Gonzalez and R. Gutierrez. Direct motion estimation from a range scan sequence. *Journal of Robotics Systems*, 16(2):73–80, 1999.

[8] A. Grossmann and R. Poli. Robust mobile robot localization from sparse and noisy proximetry readings using hough transform and probability grids. *Robotics and Autonomous Systems*, 37:1–18, 2001.

[9] D. Hähnel, D. Fox, W. Burgard, and S. Thrun. A highly efficient fastslam algorithm for generating cyclic maps of large-scale environments from raw laser range measurements. In *IEEE/RSJ International Conference on Intelligent Robots and Systems*, Las Vegas, Usa, 2003.

[10] B. Jensen and R. Siegwart. Scan alignment with probabilistic distance metric. In *Proc. of the IEEE-RSJ Int. Conf. on Intelligent Robots and Systems*, Sendai, Japan, 2004.

[11] S. Lacroix, A. Mallet, D. Bonnafous, G. Bauzil, S. Fleury, M. Herrb, and R. Chatila. Autonomous rover navigation on unknown terrains: Functions and integration. *International Journal of Robotics Research*, 21(10-11):917–942, Oct-Nov. 2002.

[12] F. Lu and E. Milios. Robot pose estimation in unknown environments by matching 2d range scans. *Intelligent and Robotic Systems*, 18:249–275, 1997.

[13] F. Lu and E. Milios. Robot pose estimation in unknown environments by matching 2d range scans. *Intelligent and Robotic Systems*, 18:249–275, 1997.

[14] J. Minguez, L. Montesano, and F. Lamiraux. Metric-based iterative closest point scan matching for sensor displacement estimation. *IEEE Transactions on Robotics (in press)*, 2006.

[15] J. Minguez, L. Montesano, and L. Montano. An architecture for sensor-based navigation in realistic dynamic and troublesome scenarios. In *IEEE Int. Conf. on Intelligent Robot and Systems*, Sendai, Japan, 2004.

[16] L. Montesano, J. Minguez, and L. Montano. Modeling the static and the dynamic parts of the environment to improve sensor-based navigation. In *IEEE International Conference on Robotics and Automation (ICRA)*, 2005.

[17] L. Montesano, J. Minguez, and L. Montano. Probabilistic scan matching for motion estimation in unstructured environments. In *IEEE Int. Conf. on Intelligent Robots and Systems (IROS)*, 2005.

[18] L. Paz, P. Piníes, J. Neira, and J. Tardós. Global localization in slam in bilinear time. In *IEEE Int. Conf. on Intelligent Robots and Systems (IROS)*, 2005.

[19] S. Pfister, K. Kreichbaum, S. Roumeliotis, and J. Burdick. Weighted range sensor matching algorithms for mobile robot displacement estimation. In *In Proceedings of the IEEE International Conference on Robotics and Automation (ICRA)*, pages 1667–74, 2002.

[20] S. Rusinkiewicz and M. Levoy. Efficient variants of the icp algorithm. In *International Conference 3DIM*, 2001.

[21] C.-C. Wang, C. Thorpe, and S. Thrun. Online simultaneous localization and mapping with detection and tracking of moving objects: Theory and results from a ground vehicle in crowded urban areas. In *Proceedings of the IEEE International Conference on Robotics and Automation (ICRA)*, 2003.